NANO LETTERS

Letter

Identifying the Length Dependence of Orbital Alignment and Contact Coupling in Molecular Heterojunctions

Jonathan A. Malen, Peter Doak, Kanhayalal Baheti, T. Don Tilley, Rachel A. Segalman, and Arun Majumdar

Nano Lett., **Article ASAP** • DOI: 10.1021/nl803814f • Publication Date (Web): 24 February 2009

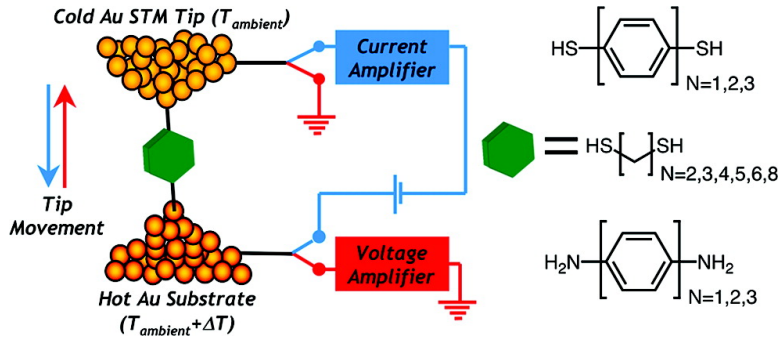

More About This Article

Additional resources and features associated with this article are available within the HTML version:

- Supporting Information
- Access to high resolution figures
- Links to articles and content related to this article
- Copyright permission to reproduce figures and/or text from this article

View the Full Text HTML

Nano Letters is published by the American Chemical Society. 1155 Sixteenth Street N.W., Washington, DC 20036

NANO LETTERS

XXXX
Vol. xx, No. x
-

Identifying the Length Dependence of Orbital Alignment and Contact Coupling in Molecular Heterojunctions

Jonathan A. Malen,[†,‡] Peter Doak,[‡,§] Kanhayalal Baheti,[§] T. Don Tilley,[§,||] Rachel A. Segalman,[*,‡,⊥,#] and Arun Majumdar[*,†,‡,⊥,▽]

Department of Mechanical Engineering, University of California, Berkeley, Berkeley, California 94720, Materials Science Division, Lawrence Berkeley National Laboratory, Berkeley, California 94720, Department of Chemistry, University of California, Berkeley, Berkeley, California 94720, Chemical Science Division, Lawrence Berkeley National Laboratory, Berkeley, California 94720, Applied Science and Technology Program, University of California, Berkeley, Berkeley, California 94720, Department of Chemical Engineering, University of California, Berkeley, Berkeley, California 94720, and Department of Materials Science and Engineering, University of California, Berkeley, Berkeley, California 94720

Received December 17, 2008

ABSTRACT

Transport in metal−molecule−metal junctions is defined by the alignment and coupling of molecular orbitals with continuum electronic states in the metal contacts. Length-dependent changes in molecular orbital alignment and coupling with contact states were probed via measurements and comparisons of thermopower (*S*) of a series of phenylenes and alkanes with varying binding groups. *S* increases linearly with length for phenylenediames and phenylenedithiols while it decreases linearly in alkanedithiols. Comparison of these data suggests that the molecular backbone determines the length dependence of *S*, while the binding group determines the zero length or contact *S*. Transport in phenylenes was dominated by the highest occupied molecular orbital (HOMO), which aligns closer to the Fermi energy of the contacts as $\sim L^{-1}$, but becomes more decoupled from them as $\sim e^{-L}$. In contrast, the decreasing trend in *S* for alkanedithiols suggests that transmission is largely affected by gold−sulfur metal induced gap states residing between the HOMO and lowest unoccupied molecular orbital.

Metal−molecule−metal junctions are the building blocks for organic and organic−inorganic hybrid materials that hold promise as inexpensive alternatives to semiconductor-based electronics, photovoltaics, and thermoelectrics.[1,2] Alignment and coupling of discrete molecular orbitals with continuum electronic states of the inorganic semiconductor component or metallic electrode create unique energy landscapes that can be precisely manipulated using chemistry. Realization of functional materials hinges on our ability to engineer these landscapes in a predictable way. Junction conductance is known to depend on molecular endgroups, backbone, and length,[3−10] but a more complete picture of the junction's electronic structure has been hitherto elusive. Least understood is the interface between the molecule and metal electrodes. Transport is defined at this interface by the alignment and coupling of molecular orbitals with mobile electrode states. Prior measurements show that the conductance of metal−molecule−metal junctions decays exponentially with molecular length, but it is unclear whether this result implies that the molecule behaves as a rectangular tunneling barrier with a fixed and discrete height. Theory indicates that this is an oversimplified picture since orbital energies depend on molecular length and the discrete levels broaden due to coupling with the electrodes.[11] Herein we present new measurements of junction thermopower (*S*) and an analytical model that together capture these effects and identify the length dependence of orbital alignment and coupling.

Charge carriers transmit through the junction with an energy-dependent probability characterized by the junction's

* Corresponding authors, majumdar@me.berkeley.edu (A.M.) and segalman@berkeley.edu (R.A.S.).
† Department of Mechanical Engineering, University of California, Berkeley.
‡ Materials Science Division, Lawrence Berkeley National Laboratory.
§ Department of Chemistry, University of California, Berkeley.
|| Chemical Science Division, Lawrence Berkeley National Laboratory.
⊥ Applied Science and Technology Program, University of California, Berkeley.
Department of Chemical Engineering, University of California, Berkeley.
▽ Department of Materials Science and Engineering, University of California, Berkeley.

10.1021/nl803814f CCC: $40.75

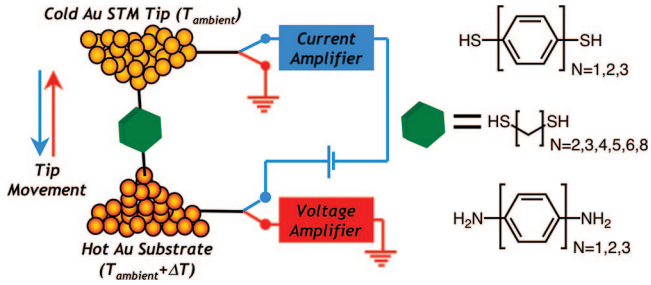

Figure 1. Experimental setup. (a) Schematic of the experimental setup for measuring the Seebeck coefficient with a modified STM break junction. *N*-unit phenylenedithiols, phenylenediamines, and alkanedithiols are captured between the Au STM tip held at ambient temperature and a heated Au substrate held at ΔT above the ambient temperature. As the STM tip advances toward the substrate, a voltage bias is applied between the tip and substrate, and current is monitored to calculate conductance. When the threshold conductance that signals the formation of a molecular junction is reached, the tip is withdrawn. During the withdrawal phase, a switch disconnects the voltage bias and current amplifier in favor of a voltage amplifier. The induced thermoelectric voltage V is measured as the tip withdraws before the junction breaks.

transmission function $\tau(E)$. In analogy to the valence and conduction bands in a semiconductor, the highest occupied molecular orbital (HOMO) and the lowest unoccupied molecular orbital (LUMO) dominate transport in a molecular junction. Transmission is peaked at the molecular orbital energies, which are not discrete in junctions, but broadened due to coupling with the continuum of states in the electrodes.[11] Since mobile carriers are present in the contacts at the chemical potential (~Fermi energy for metals, E_F), conductance (G) is related to $\tau(E)$ as follows

$$G = \frac{2e^2}{h}\tau(E)\Big|_{E=E_F} = G_0\tau(E)\Big|_{E=E_F} \quad (1)$$

where G_0 is the quantum of conductance. Hence, conductance depends on the alignment of the HOMO and LUMO with regard to E_F, as well as their broadening, which enhances transmission when E_F is off resonance from the orbitals.

Several groups have examined transport in metal−molecule−metal junctions by measuring the dependence of junction conductance on molecular length.[3−10] Conductance was found to decrease exponentially with molecular length L

$$-\beta_G = \frac{\mathrm{d}\ln G}{\mathrm{d}L} \Rightarrow G = G_C \exp(-\beta_G L) \quad (2)$$

where the scaling parameter, β_G, depends on the structure of the molecular backbone and G_C is an effective contact conductance that depends on the molecular endgroups and the electrode material. Polyaromatic molecules (e.g., phenylenes) with delocalized π-orbitals are reported to have lower β_G than saturated molecules (e.g., alkanes).[3,4,10] Hence, while conductance measurements have greatly advanced our understanding of transport at E_F, the shape of $\tau(E)$ remains unknown. Specifically, the following unanswered questions are central to understanding transport in molecular junctions: (i) Does the alignment of transmission peaks, relative to E_F, depend on molecular length? (ii) Does contact coupling broaden or narrow the transport orbitals as a function of molecular length? (iii) Is transport dominated by a single molecular orbital, or do multiple orbitals contribute? (iv)

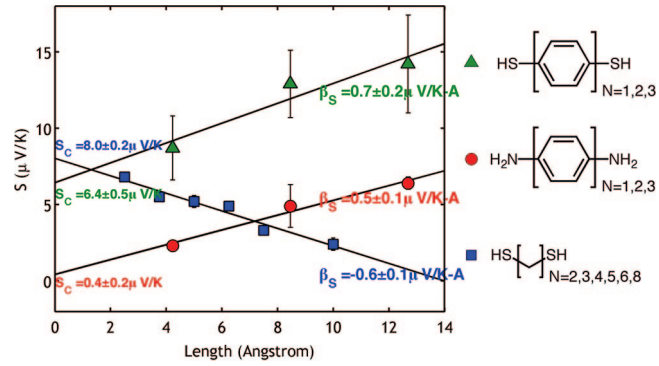

Figure 2. Seebeck coefficient vs molecular length. The Seebeck coefficient is plotted as a function of molecular length for *N*-unit phenylenedithiols ($N = 1, 2, 3$), phenylenediamines ($N = 1, 2, 3$), and alkanedithiols ($N = 2, 3, 4, 5, 6, 8$). Calculations of length are based on the molecule's length excluding endgroups with 1.25 Å per CH_2 and 4.23 Å per phenyl ring.[4] Fit lines to the data indicate that thermopower increases with length at a similar rate (β_S) for phenylenediamines and phenylenedithiols but decreases with length for alkanedithiols. In contrast, the zero-length thermopower (S_C) for phenylenedithiols and alkanedithiols is similar, while that of phenylenediamines is different. These trends suggest that β_S is related to the molecular backbone and S_C is related to the choice of endgroup.

How are components of molecular design such as endgroup and backbone related to these effects? Successful application of thermoelectricity,[12−14] rectification,[1,15] photoconductance,[16−18] light emission, and photovoltaic effects[19] require organic−metal junctions at the electrode interfaces and in some cases organic−inorganic hybrid materials as the active layer. All of these applications implore further characterization of transmission in molecular junctions.

When a temperature difference, ΔT, is applied across a metal−molecule−metal junction, a proportional voltage, V, is generated. The value of V is dictated by the junction's Seebeck coefficient or thermopower $V = S\Delta T$ is generated.[12−14] The junction Seebeck coefficient is related to $\tau(E)$ as follows

$$S = -\frac{\pi^2 k_B{}^2 T}{3e}\left(\frac{1}{\tau(E)}\frac{\mathrm{d}\tau(E)}{\mathrm{d}E}\right)\Big|_{E=E_F} = -S_0\left(\frac{1}{\tau(E)}\frac{\mathrm{d}\tau(E)}{\mathrm{d}E}\right)\Big|_{E=E_F} \quad (3)$$

where k_B is the Boltzmann constant and T is the average absolute temperature of the junction. For convenience, the intial group of constants is referred to as S_0 in analogy to eq 1. Unlike conductance, S is independent of the number of molecules in the junction and can identify the dominant transport orbital, i.e., HOMO or LUMO. Reddy and Jang found that S of phenylenedithiols increases linearly with length,[13] but the origins, implications, and generality of this result are still unknown. By examining the length dependence of S, in complement to existing G data, for alkanedithiols, phenylenedithiols, and phenylenediamines, we now identify the approximate shape of $\tau(E)$ and develop analytical relationships that predict how orbital alignment and coupling transform with molecular length, backbone, and endgroup.

Thermopower measurements were made on alkanedithiols with two, three, four, five, six, and eight CH_2 groups and phenylenediamines with one, two, and three phenyl rings. Data for phenylenedithiols with one, two, and three phenyl

Table 1. Experimental Results

	β_G (Å^{-1})	G_N[a] (G_0)	β_S (μV/(K Å))	S_C (μV/K)
phenylenediamines	0.42 ± 0.07[8]	6.4×10^{-3} ($N = 1$)[8]	0.5 ± 0.1	0.4 ± 0.2
phenylenedithiols	0.42 ± 0.07[4]	1.1×10^{-2} ($N = 1$)[20]	0.7 ± 0.2[13]	6.4 ± 0.5[13]
alkanedithiols	0.94 ± 0.06[4]	3.6×10^{-4} ($N = 6$)[6]	-0.6 ± 0.1	8.0 ± 0.2

[a] G_C can be calculated from $G_C = G_N e^{\beta_G N L_{unit}}$ and the tabulated values of G_N where $L_{unit} = 4.23$ Å for phenylenes and 1.25 Å for alkanes.

rings were reported earlier[13] and are herein referenced for comparison. A modified scanning tunneling microscope (STM), illustrated in Figure 1, was used to capture one or a few molecules for measurement of the thermoelectric voltage (experimental details are presented in Reddy et al.[13] and Baheti et al.[14]). Molecules of interest were dissolved in toluene (repeatable results were from concentrations of 0.1 mM solutions) and drop-cast onto a gold-coated mica substrate. Evaporation of the toluene solvent left the molecules bound to the gold surface. An in situ resistance heater was used to heat the substrate to ΔT above ambient (T_{AMB}), while the Au STM tip was fixed to a thermal reservoir maintained at T_{AMB}. During the STM approach process a voltage bias was applied between the tip and the substrate, and the current was monitored to calculate conductance. Prior studies indicate molecule−metal junctions have conductances on order $0.01G_0$.[20] In this study, therefore, the tip was lowered until this threshold conductance ($0.01G_0$) was reached, indicating the formation of one or a few molecular junctions. Once the junction formed, the tip was withdrawn and a switch disconnected the voltage bias and current amplifier and replaced them with a voltage amplifier. This voltage amplifier measured the induced thermoelectric voltage V as the tip withdrew before the junction broke. This process was repeated roughly 500 times at each ΔT, for $\Delta T \sim 0$, 5, 10, 15, 20, and 30 K. Histograms were built from the voltage data taken at each ΔT, without any data preselection. Histogram peaks indicate the most commonly measured voltage, V_{peak}. When plotted against ΔT, V_{peak} increases linearly with a slope equal to the thermopower of the junction, i.e., $S = V_{peak}/\Delta T$. Histograms and linear fits for each new molecule can be found in the Supporting Information. Our measurements were insensitive to the threshold conductance because S is an intensive property and, therefore, independent of the number of molecules in the junction. Equal values of S were obtained for 1,4-phenyldithiol measured with threshold conductances of $0.01G_0$, $0.1G_0$, and $1G_0$. Experimental verification is shown in the Supporting Information.

The thermopower data are plotted as a function of molecular length in Figure 2. Calculations of the molecule's length excluded the endgroups with 1.25 Å per CH_2 and 4.23 Å per phenyl ring.[4] All thermopowers were positive, indicating that $d\tau(E)/dE$ was negative at E_F from eq 3. For smoothly varying $\tau(E)$ in the region of E_F, this implies HOMO dominated transport.[12,13] Lines that were fitted to the data with least-squares analysis indicate that thermopower increases linearly with length at a similar rate for phenylenediamines and phenylenedithiols but decreases linearly with length for alkanedithiols. Extrapolation to the y-intercept shows a similar zero-length thermopower for phenylenedithiols and alkanedithiols but a different zero-length thermopower for phenylenediamines. In analogy to conductance, the rate of change of thermopower with respect to length is defined as β_S, and the zero length or contact thermopower is defined as S_C. These trends suggest that β_S is related to the molecular backbone and S_C is related to the choice of endgroup. These S data corroborate G trends, and together they clearly indicate that the length dependence of transport is related to molecular backbone, while endgroups determine the zero-length offset. The length-dependent alignment and coupling of the molecular orbitals are responsible for these trends. Values of β_S and S_C are listed in Table 1, along with referenced values of β_G and G_C.

Electron transmission based on a rectangular tunneling barrier model, originally developed by Simmons for insulating dielectric films,[21] has had reasonable success in describing the conductance of molecular junctions.[10] In this approximation

$$\beta_G(E)\Big|_{E=E_F} = 2\sqrt{\frac{2m^*}{\hbar^2}(E_F - \varepsilon_{HOMO})} \quad (4)$$

where $E-\varepsilon_{HOMO}$ is the effective barrier height assuming HOMO dominated transport and m^* is the effective mass of the tunneling electron. m^* can be interpreted as the curvature of the valance band formed by an infinite string of molecular orbitals.[22] By combining eqs 1−4, we find that

$$\beta_S(E)\Big|_{E=E_F} = \frac{dS(E)}{dL}\Big|_{E=E_F} = S_0\frac{d\beta_G(E)}{dE}\Big|_{E=E_F} = S_0\sqrt{\frac{2m^*}{\hbar^2(E_F - \varepsilon_{HOMO})}} \quad (5)$$

If β_G and β_S are known, we can uniquely identify $E-\varepsilon_{HOMO}$ and m^* from eqs 4 and 5. Values of $E-\varepsilon_{HOMO}$ and m^* for phenylenedithiols and phenylenediamines, based on the measured values of β_G and β_S, are listed in Table 1. For conjugated molecules the values of m^* are inexplicably low, and the values of $E_F-\varepsilon_{HOMO}$ are independent of length, in contrast to calculations by density functional theory and nonequilibrium Green's functions.[23,24] It is well-known that the orbital energies of conjugated molecules depend on length, so $E_F-\varepsilon_{HOMO}$ is expected to change with length. Mathematically, the Simmons model fails if β_G and β_S have opposite sign for HOMO dominated transport as is the case for alkanedithiols (or the same sign in the case of LUMO dominated transport). Hence, a rectangular barrier of this nature is inadequate to describe multiorbital transport as well as length-dependent alignment and coupling of the orbital energies. We proceed by developing a semiempirical model, with more physical resemblance to a molecular junction, based on Lorentzian-shaped transmission peaks.[11,12,25] This more complicated model will capture the broadening and alignment of the orbital energies as a function of molecular

length. The goal is a simple analytical framework that captures the transformation of $\tau(E)$ with molecular length.

Our model is derived by fitting Lorentzian transmission peaks to experimental data for G and S, which are known at E_F. Lorentzian peaks have been shown to fit the results of more advanced transmission theory for both 1,4-phenyldiamine[25] and 1,4-phenyldithiol.[12] They are accurate solutions to the junction Hamiltonian if the density of states in the contacts is constant within the energy window relevant to transport. A general expression for the Lorentzian-based transmission function is

$$\tau(E) = \sum_{n}^{N} \frac{\Gamma_{n,1}\Gamma_{n,2}}{[(\Gamma_{n,1}+\Gamma_{n,2})^2/4 + (E-\varepsilon_n)^2]} \tag{6}$$

where n indexes the molecular orbital and $\Gamma_{n,1or2}$ is the broadening in the energy of the nth orbital due to coupling with contact 1 or 2. As a consequence of the time−energy uncertainty principle ($\Delta t \Delta E = \Delta t \Gamma_{n,1or2} \sim \hbar$), $\hbar/\Gamma_{n,1or2}$ can be interpreted as the lifetime of a state in the junction before it transmits into the contacts, i.e., $\Gamma_{n,1or2}$ is proportional to the transmission rate.[11]

We focus on the orbitals that neighbor E_F—the HOMO and LUMO. Further, symmetric contacts ($\Gamma_{n,1} = \Gamma_{n,2} = \Gamma_n$), symmetric coupling of the HOMO and LUMO ($\Gamma_H = \Gamma_L$), and weak coupling ($[E_F - \varepsilon_n]^2 \gg \Gamma_2{}^n$) are assumed, which leads to the following simplified expression for transmission at $E = E_F$

$$\tau(E)\Big|_{E=E_F} = \frac{\Gamma_H{}^2}{\Delta E_H{}^2} + \frac{\Gamma_L{}^2}{\Delta E_L{}^2} \tag{7}$$

where

$$\Delta E_H = E_F - \varepsilon_{HOMO}$$
$$\Delta E_L = E_F - \varepsilon_{LUMO}$$

Next, the following ratios are defined to relate the relative distance of the HOMO and LUMO from E_F, as well as their spreads due to the contacts

$$R_{\Delta E} = \Delta E_H/\Delta E_L \tag{8}$$
$$R_\Gamma = \Gamma_L/\Gamma_H$$

where $R_{\Delta E}$ is negative because ΔE_L is negative. Substitution of (8) into (7) yields

$$G = G_0\tau(E)\Big|_{E=E_F} = \frac{G_0\Gamma_H{}^2}{\Delta E_H{}^2}(1 + R_{\Delta E}{}^2 R_\Gamma{}^2) = \frac{G_0\Gamma_H{}^2}{\Delta E_H{}^2}\rho_G \tag{9}$$

where ρ_G depends only on these ratios and is always greater than unity, thereby increasing G above its HOMO-only value. By substituting eq 6 into eq 3, the following expression for S is found

$$S = \frac{2S_0}{\Delta E_H}\left(\frac{R_{\Delta E}{}^3 R_\Gamma{}^2 + 1}{R_{\Delta E}{}^2 R_\Gamma{}^2 + 1}\right) = \frac{2S_0}{\Delta E_H}\rho_S \tag{10}$$

where ρ_S depends only on these ratios and will reduce S relative to its HOMO-only value due to contributions from the LUMO. Equation 9 suggests that conductance will be dominated by the HOMO if $\rho_G < 2$ ($R_{\Delta E}{}^2 R_\Gamma{}^2 \leq 1$), while eq 10 suggests that S will be dominated by the HOMO if $\rho_S > 0$ ($R_{\Delta E}{}^3 R_\Gamma{}^2 \geq -1$). Since all measurements of S were positive, both of these conditions are met for all molecules. If the LUMO is sufficiently far from E_F or not coupled to the contacts, then $R_{\Delta E} \to 0$ or $R_\Gamma \to 0$, and $\rho_G = \rho_S = 1$.

The observed length dependences of G and S are now used to evaluate how the HOMO's alignment, ΔE_H, and coupling, Γ_H, transform with molecular length. Expressions for G and S from eqs 9 and 10 yield

$$-\beta_G = \frac{1}{G}\frac{dG}{dL} = \frac{2}{\Gamma_H}\frac{d\Gamma_H}{dL} - \frac{2}{\Delta E_H}\frac{d\Delta E_H}{dL} + \frac{1}{\rho_G}\frac{d\rho_G}{dL} \tag{11}$$

$$\beta_S = \frac{dS}{dL} = \frac{-2S_0\rho_S}{\Delta E_H{}^2}\frac{d\Delta E_H}{dL} + \frac{2S_0}{\Delta E_H}\frac{d\rho_S}{dL} \tag{12}$$

For now, $R_{\Delta E}$ and R_Γ are assumed to be only weakly dependent on L, which implies that the HOMO and LUMO transform in proportion to one another as the molecular length is changed. This assumption should be reasonable if the composition of the HOMO and LUMO do not change with molecular length; e.g., they are composed of π orbitals that interact similarly with the contacts. Although this assumption may not be strictly true, it allows for the solution of (11) and (12) for ΔE_H and Γ_H. A less rigorous alternative that results in the same qualitative conclusions would be to entirely disregard LUMO contributions. These assumptions result in $d\rho_G/dL \sim d\rho_S/dL \sim 0$, yielding the following solutions for ΔE_H and Γ_H

$$\Delta E_H = \frac{\Delta E_{H-C}}{1 + \Delta E_{H-C}\beta_S(L - L_C)/2S_0\rho_S} \tag{13}$$

$$\Gamma_H = \frac{\Gamma_{H-C}e^{-\beta_G(L-L_C)/2}}{1 + \Delta E_{H-C}\beta_S(L - L_C)/2S_0\rho_S} \tag{14}$$

where L_C is the contact length and ΔE_{H-C} and Γ_{H-C} represent the values of ΔE_H and Γ_H for the contacts alone. These expressions are substituted back into eqs 9 and 10 resulting in analytical expressions for the length dependence of G and S

$$G = [G_0\Gamma_{H-C}{}^2\rho_G/\Delta E_{H-C}{}^2]e^{-\beta_G(L-L_C)} \tag{15}$$
$$G_C$$

$$S = [2S_0\rho_S/\Delta E_{H-C}] + \beta_S(L - L_C) \tag{16}$$
$$S_C$$

where the bracketed terms in (15) and (16) are G_C and S_C. Ultimately, the exponential decay in G results from exponential decay in contact coupling, while the linear dependence of S results from orbital alignment with E_F.

Equations 13−16 provide clear answers to our questions regarding orbital alignment and contact coupling. For phenylenediamines and phenylenedithiols, β_G and β_S are greater than zero, indicating that both ΔE_H and Γ_H decrease with L from eqs 13 and 14. This inverse relationship is expected for ΔE_H because the HOMO−LUMO gaps of isolated conjugated molecules decrease with molecular length. An electron in the delocalized orbitals of conjugated molecules behaves analogously to a particle in a box (PIB). Increased molecular length decreases the HOMO−LUMO gap just as increasing box size decreases the spacing between PIB energy levels. The exponential decay of Γ_H implies that coupling is diminished and the lifetime of junction states exponentially increases as the molecule is lengthened.

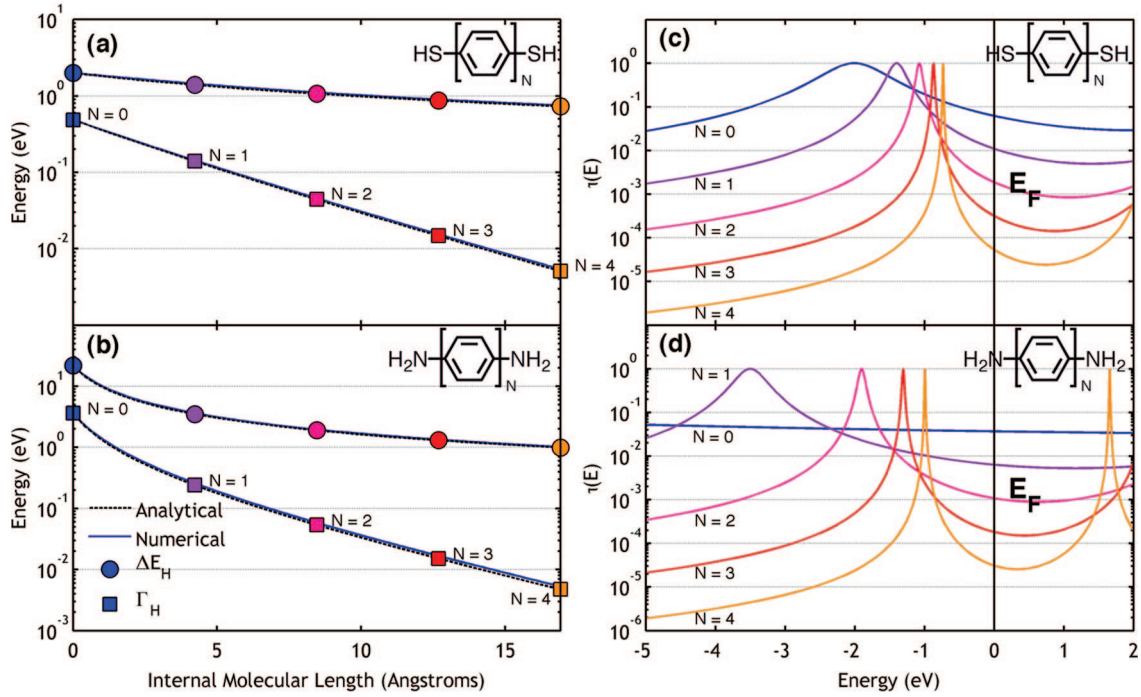

Figure 3. HOMO alignment, coupling, and transmission function vs molecular length. In subplots (a and b) the HOMO alignment with E_F (ΔE_H) and broadening due to the contacts (Γ_H) are shown as a function of molecular length for (a) phenylenedithiols and (b) phenylenediamines. The analytical results from eqs 13 and 14 based in the weak coupling limit ($[E_F - \varepsilon_n]^2 \gg \Gamma_n^2$) are compared to a numerical solution to eqs 11 and 12 that does not assume weak coupling. Points are placed at integer molecular units (N). Lorentzian based transmission functions for N-unit molecules are shown in the adjacent subplots, for (c) phenylenedithiols and (d) phenylenediamines. Color coordinated curves match the points in the adjacent subplots (a and b). As molecular length is increased, the HOMO peak aligns closer to E_F as $\sim L^{-1}$ and narrows in width due to reduced coupling as $\sim e^{-L}$. The observed trends in thermopower and conductance result from the combined length dependence of orbital alignment and contact coupling.

Table 2. Modeling Parameters

	Simmons model		Lorentzian model					
	$E_F - E_{HOMO}$ (eV)	m^*/m_e	$R_{\Delta E}{}^a$	$R_\Gamma{}^b$	ρ_G	ρ_S	ΔE_{H-C} (eV)	Γ_{H-C} (eV)
phenylenediamines	3.2 ± 0.8	0.05 ± 0.01	-0.6[25]	1.0	1.36	0.57	21.8	3.6
phenylenedithiols	2.4 ± 0.9	0.07 ± 0.03	-0.33[12,29]	1.0	1.11	0.87	2.0	0.48

[a] Values based on HOMO−LUMO gap from referenced transmission functions. [b] Values assumed based on equivalent coupling of the HOMO and LUMO to the contacts.

Equations 13−16 are tools for molecular design that can be roughly applied, with knowledge of backbone and endgroup, in the absence of complicated DFT and NEGF calculations. They represent a distinct improvement over the rectangular barrier model because they capture the anticipated length dependence of orbital alignment and contact coupling.

Plots of ΔE_H and Γ_H for phenylenediamines and phenylenedithiols are shown in Figure 3, panels a and b. The numerical solution to eqs 11 and 12, shown as blue solid lines, was computed without the assumption of weak coupling. It is accurately matched by eqs 13 and 14, proving that this was a good assumption for these systems. Data from G and S measurements lead to the values of ΔE_{H-C} and Γ_{H-C} listed in Table 2. Values of $R_{\Delta E}$ and R_Γ listed in Table 2 were found by inspection of transmission functions found in existing literature. The qualitative behavior of ΔE_H and Γ_H is identical if the LUMO's effect is negated by setting these values equal to zero. The calculated Lorentzian based transmission functions for phenylenediamines and phenylenedithiols with zero to four phenyl rings are shown in Figure 3, panels c and d. The color-coded curves are defined by (6), where the values of ΔE_H and Γ_H are correspondingly colored in Figure 3, panels a and b. In general, the HOMO peak narrows and moves toward E_F as the molecular length is increased. Comparison of curves with equal N for phenylenedithiols and phenylenediamines indicates that the thiol HOMO is closer to E_F, while the amine HOMO peak is more broadened. The employed values of $R_{\Delta E}$ and R_Γ suggest that the LUMO is more influential to amine transport, resulting in increased G and decreased S relative to their HOMO-only values.

Alkanedithiols exhibit negative β_S, which from eq 13 leads to the unexpected conclusion that ΔE_H increases with L. The HOMO−LUMO gap of isolated nonconjugated molecules typically remains constant with molecular length. Here the PIB argument does not apply because the orbitals are localized and the addition of new orbitals does not affect existing states. Instead, the observed negative β_S is related to the presence of additional states in the HOMO−LUMO gap that are composed mainly of gold and sulfur orbitals mixed with the localized orbitals of the alkane chain. These states, known as metal induced gap states (MIGS), have

already been suggested by theory[23,26,27] and observed in experiments.[28] The extent to which MIGS effect junction transmission was hitherto indiscernible by junction conductance measurements. Although junction conductance is affected by gap states, it is difficult to separate their effect from that of the HOMO. Both the sign and magnitude of thermopower can be affected by the presence of MIGS. In the framework developed above, one can replace LUMO contributions with contributions from a gap state. The HOMO and MIGS transform differently with molecular length since their orbital compositions are very different. Theory suggests that when the molecule is short, the gap states dominate, but when the molecule is long, their contribution is negligible.[23,27] Hence, within eq 12, $d\rho_S/dL \neq 0$, and its value can influence the length dependence of thermopower. We speculate that the negative β_S results from inequity in length dependence of the MIGS and the HOMO.

In summary, length-dependent changes in molecular orbital alignment and coupling with contact states were probed via measurements of thermopower (S) on a series of phenylenediamines, phenylenedithiols, and alkanedithiols trapped between gold contacts. S increases linearly with length for phenylenediames and phenylenedithiols while it decreases linearly in alkanedithiols. Comparison of these data suggests that the molecular backbone determines the length dependence of S, while the endgroup determines the zero-length, or contact S. Due to the inadequacies of a simple rectangular barrier model, a new model based on the observed length dependence of thermopower and conductance was developed to understand these trends. This model captures length-dependent changes in orbital alignment and contact coupling, which, when combined, result in the observed trends in S and G. Specifically, for phenylene backboned molecules, the HOMO dominates transport and moves closer to E_F but becomes more decoupled from the contacts, as molecular length is increased. This transformation of the transmission function results in the observed reduction in conductance and increase in thermopower. Contributions from the LUMO are more influential for phenylenediamines than phenylenedithiols and act to increase conductance but decrease thermopower relative to the HOMO-only values. The thermopower of alkanedithiols decreases with length, because transmission is largely effected by gold−sulfur metal induced gap states between the HOMO and LUMO.

Acknowledgment. We gratefully acknowledge support from the Division of Materials Sciences and Engineering in the Department of Energy Basic Energy Sciences (DOEBES) through the Helios Program at Lawrence Berkeley National Laboratory (LBNL). We also gratefully acknowledge support in the form of instrumentation from the NSF-NSEC-COINS at UC Berkeley. We thank J. B. Neaton and Su Ying Quek from LBNL, as well as S. Yee from UC Berkeley, for insightful conversations that benefited this work.

Supporting Information Available: Thermoelectric voltage histograms and data analysis methods. This material is available free of charge via the Internet at http://pubs.acs.org.

References

(1) Joachim, C.; Gimzewski, J. K.; Aviram, A. *Nature* **2000**, *408* (6812), 541–548.
(2) Love, J. C.; Estroff, L. A.; Kriebel, J. K.; Nuzzo, R. G.; Whitesides, G. M. *Chem. Rev.* **2005**, *105* (4), 1103–1169.
(3) Beebe, J. M.; Engelkes, V. B.; Miller, L. L.; Frisbie, C. D. *J. Am. Chem. Soc.* **2002**, *124* (38), 11268–11269.
(4) Wold, D. J.; Haag, R.; Rampi, M. A.; Frisbie, C. D. *J. Phys. Chem. B* **2002**, *106* (11), 2813–2816.
(5) Xu, B. Q.; Tao, N. J. J. *Science* **2003**, *301* (5637), 1221–1223.
(6) Jang, S. Y.; Reddy, P.; Majumdar, A.; Segalman, R. A. *Nano Lett.* **2006**, *6* (10), 2362–2367.
(7) Tao, N. J. *Nat. Nanotechnol.* **2006**, *1* (3), 173–181.
(8) Venkataraman, L.; Klare, J. E.; Nuckolls, C.; Hybertsen, M. S.; Steigerwald, M. L. *Nature* **2006**, *442* (7105), 904–907.
(9) Venkataraman, L.; Klare, J. E.; Tam, I. W.; Nuckolls, C.; Hybertsen, M. S.; Steigerwald, M. L. *Nano Lett.* **2006**, *6* (3), 458–462.
(10) Engelkes, V. B.; Beebe, J. M.; Frisbie, C. D. *J. Am. Chem. Soc.* **2004**, *126* (43), 14287–14296.
(11) Datta, S. *Quantum transport: atom to transistor*; Cambridge University Press: Cambridge, U.K., and New York, 2005; pp xiv and 404.
(12) Paulsson, M.; Datta, S. *Phys. Rev. B* **2003**, *67* (24), 241403.
(13) Reddy, P.; Jang, S. Y.; Segalman, R. A.; Majumdar, A. *Science* **2007**, *315* (5818), 1568–1571.
(14) Baheti, K.; Malen, J. A.; Doak, P.; Reddy, P.; Jang, S. Y.; Tilley, T. D.; Majumdar, A.; Segalman, R. A. *Nano Lett.* **2008**, *8* (2), 715–719.
(15) Aviram, A.; Ratner, M. A. *Chem. Phys. Lett.* **1974**, *29* (2), 277–283.
(16) Galperin, M.; Nitzan, A.; Ratner, M. A. *Phys. Rev. Lett.* **2006**, *96* (16), 166803.
(17) Viljas, J. K.; Cuevas, J. C. *Phys. Rev. B* **2007**, *75* (7), 075406.
(18) Viljas, J. K.; Pauly, F.; Cuevas, J. C. *Phys. Rev. B* **2007**, *76* (3), 155119.
(19) Galperin, M.; Nitzan, A. *Phys. Rev. Lett.* **2005**, *95* (20), 206802.
(20) Xiao, X. Y.; Xu, B. Q.; Tao, N. J. *Nano Lett.* **2004**, *4* (2), 267–271.
(21) Simmons, J. G. *J. Appl. Phys.* **1963**, *34* (6), 1793.
(22) Tomfohr, J. K.; Sankey, O. F. *Phys. Rev. B* **2002**, *65* (24), 245105.
(23) Crljen, Z.; Grigoriev, A.; Wendin, G.; Stokbro, K. *Phys. Rev. B* **2005**, *71* (16), 165316.
(24) Xue, Y. Q.; Ratner, M. A. *Phys. Rev. B* **2003**, *68* (11), 115406.
(25) Quek, S. Y.; Venkataraman, L.; Choi, H. J.; Loule, S. G.; Hybertsen, M. S.; Neaton, J. B. *Nano Lett.* **2007**, *7* (11), 3477–3482.
(26) Kaun, C. C.; Guo, H. *Nano Lett.* **2003**, *3* (11), 1521–1525.
(27) Zhou, Y. X.; Jiang, F.; Chen, H.; Note, R.; Mizuseki, H.; Kawazoe, Y. *J. Chem. Phys.* **2008**, *128* (4), 044704.
(28) Zeng, C. G.; Li, B.; Wang, B.; Wang, H. Q.; Wang, K. D.; Yang, J. L.; Hou, J. G.; Zhu, Q. S. *J. Chem. Phys.* **2002**, *117* (2), 851–856.
(29) Stokbro, K.; Taylor, J.; Brandbyge, M.; Mozos, J. L.; Ordejon, P. *Comput. Mater. Sci.* **2003**, *27* (1−2), 151–160.

NL803814F